High Image Quality Wearable Displays with a Fast-response Liquid Crystal

Zhenyue Luo*, Fenglin Peng*, Haiwei Chen*, Minggang Hu**, and Shin-Tson Wu*

*College of Optics and Photonics, University of Central Florida, Orlando, Florida 32816, USA

**Xi'an Modern Chemistry Research Institute, Xi'an 710065, China

Abstract

We report two ultra-low viscosity liquid crystals for high image quality wearable displays with a field sequential color LCOS. Our mixtures offer ~4X faster response time than a commercial material at 20°C and ~8X faster at −20°C. Such a fast response time offers vivid color, high ambient contrast ratio, low power consumption, and mitigated color breakup even at -20°C. Different LC modes and frame rates are also evaluated.

1. Introduction

Field sequential color liquid-crystal-on-silicon (FSC-LCOS) has been widely used in wearable displays, such as near-eye display (Google Glass) and smart watches [1-3]. FSC offers high brightness, excellent ambient contrast ratio, and low power consumption. However, a wearable display needs to work in a wide outdoor temperature range. FSC-LCOS would suffer from poor image quality at low temperatures where the LC response time is sluggish and the color mixing is severe [4-6]. One way to resolve this issue is to implement an extra heater to elevate the operation temperature [5], but this approach greatly increases the power consumption.

In this paper, we propose two new ultra-low viscosity LC materials for FSC-LCOS. Compared to commercial LC materials, our materials show 4X faster response time at 20°C and 8X faster at -20°C. It overcomes the color mixing issue without heating up the device. Meanwhile, it enables high frame rate driving to suppress the color breakup artifact. These ultra-low viscosity LCs offer high image quality for wearable displays even at low temperatures.
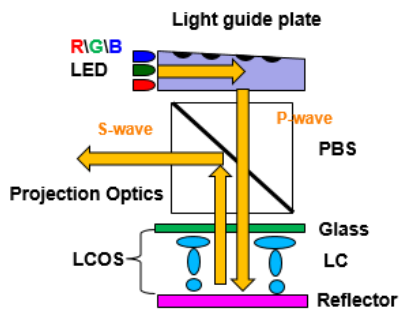
2. Color Mixing Effect

Figure 1. Schematic of LCOS module for near-eye display

Figure 1(a) shows a typical LCOS scheme for near-eye display such as Google Glass. The R/G/B LEDs are turned on and off sequentially, the polarization beam splitter (PBS) controls the light path through polarization, and the LCOS modulates grey levels by varying the light polarization state. Figure 2(a) illustrates the mechanism of color mixing effect between red and green. During the transition, if the LC response time is too slow,

then the red field would extend to the green field. This green light leakage deteriorates the color purity of red, and accordingly reduces the displayed color gamut. Figure 2(b) shows the color gamut shrinkage using a commercial LC material (JC1041). The color gamut is shrunk by 21% at 0°C and 62% at -10°C. At -20°C, the decay/rise time of JC0141 is [3.1ms, 26.4ms], which is significantly longer than a single color frame (5.55ms for 180Hz). Therefore, as the ambient temperature decreases, conventional FSC-LCOS suffers from severe degradation in color gamut because of the slow LC response time.
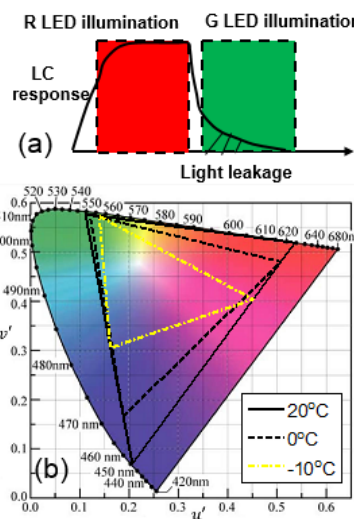

Figure 2. (a) Origin of color mixing effect. (b) Reduced color gamut at low temperatures with a commercial LC material (JC1041) at 180Hz driving and 90% LED duty.

3. Material Improvement & Device Simulation

The response time of LCOS is given as: $t \sim \gamma_1 d^2 / K\pi^2$. where d is the cell gap, γ_1 is the rotational viscosity, and K the effective elastic constant. γ_1 increases exponentially as the temperature decreases: $\gamma_1 \sim exp(E/k_B T)$, where E is the activation energy and k_B the Boltzmann constant [7]. To achieve fast response time at low temperature, three approaches can be considered: thin cell gap d, small γ_1/K, and low activation energy E. Although thin cell gap helps reduce response time [8-9], a minimal $d\Delta n$ value is needed in order to achieve high reflectance. That means, a thinner cell gap should be compensated by a higher birefringence. Indeed, some high Δn LC materials have been reported to improve the response time of a VA LCOS [9]. A big challenge of the thin cell gap approach is its compromised manufacturing yield. Blue phase liquid crystal (BPLC) has also been explored because of its submillisecond response time and

Table 2. Physical properties of three LC mixtures studied. T= 23°C and f = 1 kHz.

	20°C			0°C			−20°C			E (meV)	T_c (°C)
	$\Delta\varepsilon$	Δn	γ_1/K_{11}	$\Delta\varepsilon$	Δn	γ_1/K_{11}	$\Delta\varepsilon$	Δn	γ_1/K_{11}		
JC-1041	6.1	0.145	15.6	6.6	0.151	28.6	7.0	0.157	110	370	91
UCF-L2	3.1	0.122	3.9	3.7	0.127	7.3	4.2	0.133	14.5	227	80
DIC-LC2	2.0	0.121	2.6	2.5	0.128	4.9	3.1	0.135	9.0	180	75

insensitivity to cell gap [10, 11]. However, the Kerr constant and response time of BPLC are sensitive to the temperature, especially in the low temperature region [12].

Instead of seeking high birefringence material, in this paper we investigated LC materials with ultra-low viscosity and smaller activation energy E. At low temperature, the viscosity γ_1 exponentially increases and governs the LC response. Smaller activation energy E can significantly suppress the increasing rate of γ_1 [13,14]. Therefore, low viscosity γ_1 and smaller activation energy E are effective for reducing the response time at low temperatures.

To formulate an ultra-low viscosity LC mixture, we prepared some high Δn and large $\Delta\varepsilon$ compounds whose $\Delta\varepsilon$ value is as large as 25. Table 1 lists the chemical structures and compositions of our mixture, designated as UCF-L2. Compounds 1 and 2 have high Δn and large $\Delta\varepsilon$ [14, 15], but their viscosity is relatively high. To lower the viscosity, we added 53% diluters [17] whose structure is also included in Table 1 (#3). For practical applications, an LC mixture should exhibit a wide nematic range and high clearing point, thus we added 22% terphenyl compounds (#4) to widen the nematic range.

Table 1. Chemical structures and compositions of UCF-L2; R and R' represent alkyl chains.

| No.	Compound Structure	wt%
1		15%
2		10%
3		53%
4		22%

In addition to UCF-L2, we also evaluate the LCOS performance using another ultra-low viscosity LC mixture (DIC-LC2) reported in Ref. [15]. Table 2 lists the physical properties of JC-1041, UCF-L2, and DIC-LC2 at three temperatures: 20°C, 0°C, and −20°C. Among these three mixtures, JC-1041 has the highest $\Delta\varepsilon$, Δn, and clearing point, but its γ_1/K_{11} is also the largest. In addition, JC-1041 has a relatively high activation energy ($E\sim370$meV), which implies that its γ_1/K_{11} increases

substantially as the temperature decreases. In contrast, UCF-L2 and DIC-LC2 have smaller dielectric anisotropy and birefringence, but their γ_1/K_{11} and activation energy are also much lower. From Table 2, the γ_1/K_{11} value of DIC-LC2 is ~5X smaller than that of JC-1041 at 20°C and ~12X at −20°C. UCF-L2 and DIC-LC2 have a lower clearing temperature than JC-1041, but they are still sufficient for most outdoor applications. Among the two low-viscosity materials studied, UCF-L2 has a slightly higher γ_1/K_{11} than DIC-LC2, but its $\Delta\varepsilon$ is also larger so that its operation voltage is lower.
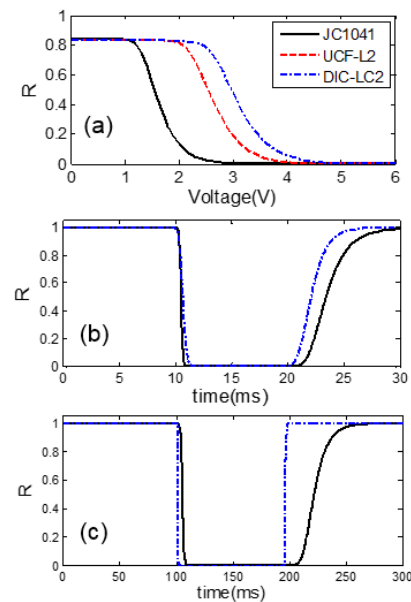
Figure 3. (a) Simulated VR curves (λ=550nm) of MTN-90° cells using three LC mixtures. (b) and (c) Dynamic response curves of JC-1041 and DIC-LC2 at 20°C and −20°C, respectively.

Based on the experimental LC parameters, we simulated the LCOS with normally white 90° mixed-mode twisted nematic (MTN-90°) mode [8]. MTN-90° mode is popular in LCOS display due to its high contrast ratio, low operation voltage, small fringe field effect, and no need for a compensation film. Fig. 3(a) plots the voltage dependent reflectance. For fair comparison, we fixed $d\Delta n$=220nm all three materials. There is a clear trade-off between γ_1 (response time) and $\Delta\varepsilon$ (operating voltage). For example, DIC-LC2 has the lowest viscosity, but its dielectric anisotropy is the smallest, meaning it needs a higher voltage (~5V) to achieve good dark state. Currently, most LCOS

electronic drivers can supply more than 5V, so the operating voltage for DIC-LC2 is still acceptable. Figure 3(b,c) compares the LCOS dynamic response at 20°C and −20°C respectively. The dynamic response of UCF-L2 is very close to that of DIC-LC2 and therefore not shown in the figure. It is evident that DIC-LC2 has much faster response time than JC-1041, and this advantage is more pronounced in the low temperature region because of its low activation energy.
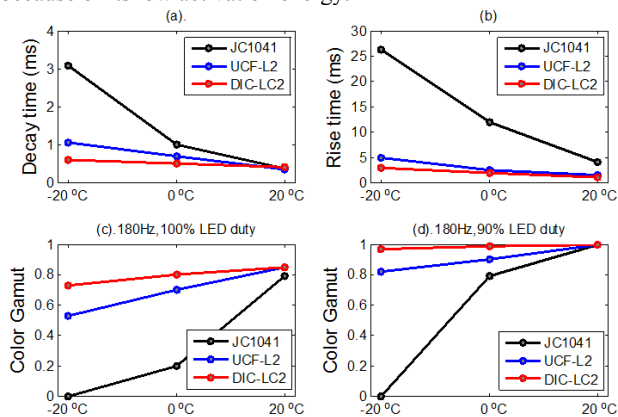
Figure 4. (a,b) LC decay and rise time at different temperatures. (c,d) Color gamut ratio for 180Hz frame rate with 100% LED rate and 90% LED rate, respectively.

Figure 4(a,b) compares the decay time and rise time for different LCOS materials. Among all three LC materials, DIC-LC2 manifests the fastest decay/rise time. At 20°C, its total response time (rise + decay) is 1.52ms, which is 4X faster than that of JC1041. Compared to JC1041, UCF-L3 also shows a slower increasing rate at low temperatures. At −20°C, the total response time of DIC-LC2 is ~3.55ms, which is 8X faster than that of JC1041. This dramatic response time improvement is beneficial to reduce color mixing and color breakup artifacts.

We also simulated the color gamut shrinkage effect by taking integration of LC response curve in the time domain [14]. Fig. 4(c) shows the case for 180Hz frame rate and 100% LED duty. The color gamut is normalized to LED color gamut in CIE1976 color space. The color gamut of JC1041 is 79% at 20°C, but quickly shrinks to 17% at 0°C and 0% and -20°C. On the other hand, DIC-LC2 shows 85% color gamut at 20°C and still maintains 73% color gamut at -20°C. The LCOS image quality can still be well preserved even at low temperatures.

Reducing the LED turn-on duty is another way to suppress color mixing effect as it increases the temporal separation of each color field. Fig. 4(d) is a plot of the color gamut ratio for 180Hz frame rate and 90% LED duty. The temporal separation is 0.55ms. At 20°C, all three LC materials can obtain ~100% color gamut since LC decay time is less than 0.55ms. However, as the temperature decreases the JC1041 color gamut starts to decrease significantly. In comparison, DIC-LC2 can still maintain 97% color gamut coverage at -20°C. Usually LED color gamut can covers >110% NTSC, therefore we can achieve 110%*97%=106.7% color gamut even at low temperature. This vivid color is very attractive for wearable display as it also improves the ambient contrast ratio.

We also studied the effect of increased frame rate. High frame rate is effective to suppress the color breakup artifact in FSC displays, but it introduces more severe color mixing and

accordingly reduces the color gamut if the LC response time is not fast enough [18]. Commercial LC material is too slow to support high frame driving. In comparison, Fig. 5(a) plots the color gamut ratio of our DIC-LC2 with increased frame rate. Even with 360Hz frame rate, our DIC-LC2 can still provide >95% color gamut at 20°C and >60% color gamut at -20°C. Therefore, color breakup can be suppressed without sacrificing the image quality.
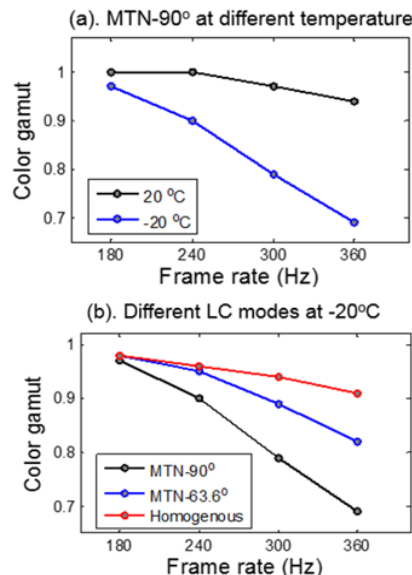
Figure 5. (a) Color gamut coverage of MTN-90° mode at different temperatures and driving frequencies. (b) Color gamut coverage of different LC modes at -20°C. LC material is DIC-LC2 and 90% LED duty ratio.

Finally, we investigated the influence of different LC modes. Form Fig. 2(a), the image decay process is more ciritical to color mixing effect as it introduces light leakage from next sub-frame. A normally-white LCOS is favorable for projection display because of its voltage-assisted fast decay process. Fig. 5(b) compares three types of normally-white LC modes: 90° mixed-mode twisted nematic (MTN-90°) , 63.6° mixed-mode twisted nematic mode (MTN-63.6°) as well as film-compensated homogenous cell [1]. Their cell gap dΔn equals to 220nm, 200nm, and 185nm respectively. In the voltage-on state their reflectance ~80%. Fig. 5(b) compares their color gamut ratio at different frame rates. Homogenous mode has the fastest response time due to its thinnest cell gap. As a result, the homogenous mode can maintain 90% color gamut even at 360Hz and at -20°C. The decay/rise time of homogenous mode is [0.33ms, 0.61ms] at 20°C and [0.53ms, 1.43ms] at -20°C. This response time is even faster than that of blue phase projection displays [10,11], but with much lower driving voltage. A drawback of MTN-63.6° and homogenous cells is that they require a phase compensation film in order to obtain good dark state. As the temperature varies, the dark state voltage would drift slightly because the birefringence of LC changes more quickly than that of compensation film. Despite of this problem, they are still attractive especially when dynamic response is the major concern.

4. Summary

We have developed two LC mixtures with ultra-low viscosity. These new LCs exhibit several attractive features for field sequential color LCOS: (1) Vivid color image even at -20°C and sub-millisecond response LC time at room temperature. (2) Ultra-low power consumption by avoiding the device heating process. (3) High brightness and excellent ambient contrast ratio. (4) Suppressed color breakup with higher frame rate driving and fast LC response time. (5) Compact module by integration with front-lighting technique. This fast response LCOS is promising for next-generation wearable displays.

5. References

[1] D. Armitage, I. Underwood, and S. T. Wu, *Introduction to Microdisplays* (Wiley, 2006).

[2] M. S. Brennesholtz and E. H. Stupp, *Projection Displays*, 2nd Ed. (Wiley, 2008).

[3] D. Cuypers, H. De Smet, and A. Van Calster, "VAN LCOS Microdisplays: A Decade of Technological Evolution," J. Display Technol. **7**, 127-134 (2011).

[4] J. Bergquist and C. Wennstam, "49.2: Field-Sequential-Colour Display with Adaptive Gamut," SID Dig. Tech. Papers **37**, 1594-1597 (2006).

[5] K.-H. Fan-Chiang, C.-C. Lai, J.-T. Cheng, C.-C. Yen, B.-J. Liao, Y.-Y. Ho, and Y.-C. Chen, "P-173: A 0.38" Field-Sequential-Color Liquid-Crystal-On-Silicon Microdisplay for Mobile Projectors," SID Dig. Tech. Papers **40**, 1770-1773 (2009).

[6] Y.-W. Li, K.-H. Fan-Chiang, C.-T. Wang, C.-L. Wu, C.-Y. Tsai, H.-C. Tsai, and H.-C. Huang, "P-121: Fast-Response Reflective TN Mode with Enhanced Contrast and Reflectance," SID Dig. Tech. Papers **41**, 1720-1723 (2010).

[7] S. T. Wu and C. S. Wu, "Rotational viscosity of nematic liquid crystals: A critical examination of existing models," Liq. Cryst. **8**, 171-182 (1990).

[8] S. T. Wu and C. S. Wu, "Mixed-mode twisted nematic liquid crystal cells for reflective displays," Appl. Phys. Lett. **68**, 1455-1457 (1996).

[9] Y. Chen, F. Peng, and S. T. Wu, "Submillisecond-Response Vertical-Aligned Liquid Crystal for Color Sequential Projection Displays," J. Display Technol. **9**, 78-81 (2013).

[10] S. He, J.-H. Lee, H.-C. Cheng, J. Yan, and S.-T. Wu, "Fast-Response Blue-Phase Liquid Crystal for Color-Sequential Projection Displays," J. Display Technol. **8**, 352-356 (2012).

[11] L. Rao, S. He, and S.-T. Wu, "Blue-phase liquid crystals for reflective projection displays," J. Display Technol. **8**, 555-558 (2012).

[12] F. Peng, Y. Chen, J. Yuan, H. Chen, S.-T. Wu, and Y. Haseba, "Low temperature and high frequency effects on polymer-stabilized blue phase liquid crystals with large dielectric anisotropy," J. Mater. Chem. C **2**, 3597-3601 (2014).

[13] H. Chen, F. Peng, Z. Luo, D. Xu, S. T. Wu, M. Li, S. Lee, and W. Tsai, "High performance liquid crystal displays with a low dielectric constant material," Opt. Mater. Express **4**, 2262-2273 (2014).

[14] Z. Luo, F. Peng, H. Chen, M. Hu, J. Li, Z. An, and S.T. Wu, "Fast-response liquid crystals for high image quality wearable displays," Opt. Mater. Express **5**, 603-610 (2015)

[15] H. Takatsu, "Advanced Liquid Crystal Materials for Active Matrix Displays," Conf. Proc. Advanced Display Materials and Devices, p.43 (Sendai, Japan, 2014).

[16] J. Li, M. Hu, J. Li, Z. An, X. Yang, Z. Yang, and Z. Che, "Highly fluorinated liquid crystals with wide nematic phase interval and good solubility," Liq. Cryst. **41**, 1783-1790 (2014).

[17] M. Schadt, R. Buchecker, and K. Muller, "Material properties, structural relations with molecular ensembles and electro-optical performance of new bicyclohexane liquid crystals in field-effect liquid crystal displays," Liq. Cryst. **5**, 293-312 (2014).

[18] Z. Luo and S.T. Wu, "A Spatiotemporal Four-Primary Color LCD with Quantum Dots," J. Display Technol. **10**, 367-372 (2014).